A Radiation Monitor for Future Space Missions

Patrícia Gonçalves, Mário Pimenta and BernardoTomé[1]

***Abstract*—A study of a baseline configuration for a next generation of light, compact and low power consuming radiation monitors for future space missions is presented. The instrument concept developed performs not only as a radiation switch, providing ancillary radiation environment information to the spacecraft, but also as a scientific instrument, capable of measuring electrons with energies between 100 keV and 20 MeV, and protons and ions with energies ranging between 0.5 MeV and 150 MeV. The studies reported depart from a Geant4 simulation of a baseline design based on a scintillating crystal and on a two plane silicon tracker**

I. Introduction

Radiation monitors are becoming an essential component in space missions, providing crucial radiation environment information for the in-flight protection of the spacecraft and instruments onboard. In addition, the data acquired during the mission are valuable inputs for space environment models; in particular data gathered in missions to other planets (e.g. particle fluxes and spectral distributions as a function of the distance to the Sun) are essential for models describing the injection and propagation of particles from the Sun. Several of the future space missions (e.g. LISA, Gaia, JWST, Bepi-Colombo) are planned to carry radiation monitors. Given the limited resources on mass, power and accommodation onboard a spacecraft, a new generation of compact and lightweight general purpose energetic particle detectors are being explored.

Monte Carlo simulation tools are essential to develop and optimize a given detector concept and to explore alternative detector concepts. The ability to predict the detector performance in realistic radiation environments is also crucial. This requires the implementation of software models in order to perform an end-to-end simulation, including particle propagation from the source to the spacecraft location, followed by a detailed simulation of the detector response.

The Geant4 toolkit is an ideal framework for simulating particle interactions with detector materials in complex geometries. A Geant4 based simulation of a compact lightweight radiation monitor concept for future space missions is presented.

[1]This work was supported in part by the FCT grants SFRH/BPD/11500/2002 and SFRH/BPD/11547/2002. Authors are with LIP - Laboratório de Instrumentação e Física Experimental de Partículas, Av. Elias Garcia, nº14,1º Lisboa, 1000-149, Portugal.

II. Space Radiation Environment

The high energy ionizing radiation[2] environment in the solar system consists of three main sources: the radiation belts, galactic cosmic rays and solar energetic particles.

The radiation belts are composed of electrons and protons trapped in the magnetosphere of the planets. In Earth's radiation belts (Van Allen belts), electrons have energies smaller than about 6-10 MeV and protons have energies up to 250 MeV [1]. Earth's radiation belts are mostly relevant for low earth orbit (LEO) missions.

The galactic cosmic rays (GCR) component consists of a continuous flux of electrons, protons and ions, arriving from beyond the solar system, which are originated mainly in the supernovae. The GCR flux is maximal at energies around 1 GeV/n, decreasing as a power law for higher energies. Lower energy particles are strongly affected by the 11-year solar cycle. Although the GCR flux is comparatively low, energetic heavy ions can locally produce significant energy depositions originating single-event upsets.

Solar energetic particle events (SPE) consist of a sudden and dramatic increase in the flux of particles from the sun, including electrons, protons and heavier ions. SPE are associated with impulsive solar flares and Coronal Mass Ejections and occur with higher probability during the solar cycle maxima. Although the energies of SPE rarely exceed few hundred MeV they give rise to potential risks for space missions due to the high fluxes attained. On the other hand their study is relevant for developing and testing solar particle propagation models [2].

III. The GEANT4 toolkit

Geant4 [3,4] is a Monte Carlo radiation transport simulation toolkit, with applications in areas as high energy physics, nuclear physics, astrophysics or medical physics research. It follows an Object-Oriented design which allows for the development of flexible simulation applications. Geant4 includes an extensive set of electromagnetic, hadronic and optics physics processes and tracking capabilities in 3D

[2] In the context of space radiation effects, particles are considered energetic if their energy is high enough to penetrate the outer skin of the spacecraft. This means electrons with energies above 100 keV, protons and ions with energies above 1 MeV.

geometries of arbitrary complexity. The electromagnetic physics category covers the energy range from 250 eV to 10 TeV (up to 1000 PeV for muons) while hadronic physics models span over 15 orders of magnitude in energy, starting from neutron thermal energies. The optical physics process category allows the simulation of scintillation, Cherenkov or transition radiation based detectors. A distinct class of particles, the optical photons, is associated to this process category. The tracking of optical photons includes refraction and reflection at medium boundaries, Rayleigh scattering and bulk absorption.

The optical properties of a medium, such as refractive index, absorption length and reflectivity coefficients, can be expressed as functions of the photon's wavelength. The characteristics of the interfaces between different media can be defined using the UNIFIED optical model [5]. Full characterisation of scintillators include emission spectra, light yields, fast and slow scintillation components and associated decay time constants.

IV. Simulation of a Generic Space Radiation Monitor Concept

The simulation of a simple space radiation monitor concept [6] was implemented using the Geant4 toolkit. The detector consists of a tracker made of two position sensitive silicon planes followed by a CsI(Tl) scintillating crystal surrounded by photodetectors (Fig.1).

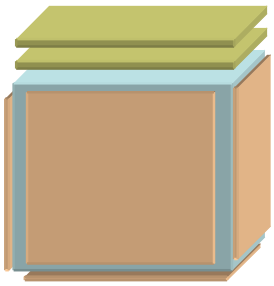

Fig. 1 View of the simulated particle detector. From top to bottom: the two silicon planes and the scintillating crystal surrounded by 5 photodetectors.

In the present simulation the silicon tracker planes were 500 μm thick, the crystal size was 3x3x3 cm^3 thick. The scintillation properties of the CsI(Tl) crystal were used. These included a light yield of 65000 photons per MeV of deposited energy and two scintillation components with decay time constants of 0.68 μs (64%) and 3.34 μs (36%). The scintillation light is readout by large area silicon PIN photodiodes, with a spectral sensitivity matching the CsI(Tl) emission spectrum. Since the silicon photodiodes are sensitive both to photons and charged particles, this makes them suitable to be used also as anti-coincidence shield.

Particle identification is performed by measuring the energy loss in the thin silicon trackers. Figure 2 shows the simulated energy loss in the first (top) and second (bottom) silicon planes, as a function of the initial particle energy, for electrons, protons and alphas. Figure 3 shows the energy deposited in the crystal by electrons, protons and alpha particles as a function of their kinetic energy before entering the detector.

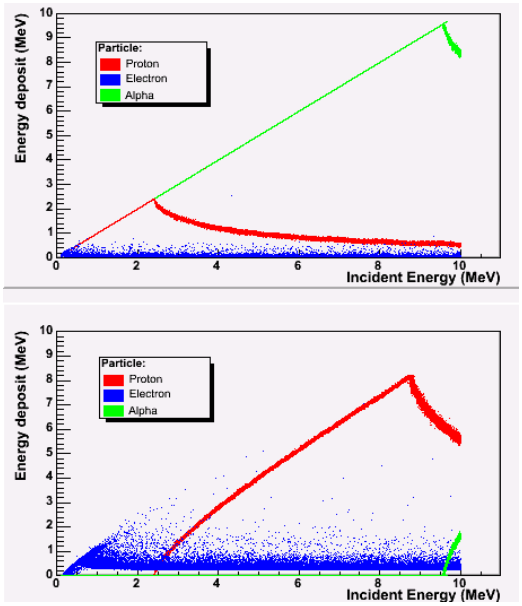

Fig. 2 Energy deposited in the first (top) and second (bottom) tracker planes by electrons (blue dots), protons (red dots) and alpha particles (green dots), as a function of the energy of the incoming particle.

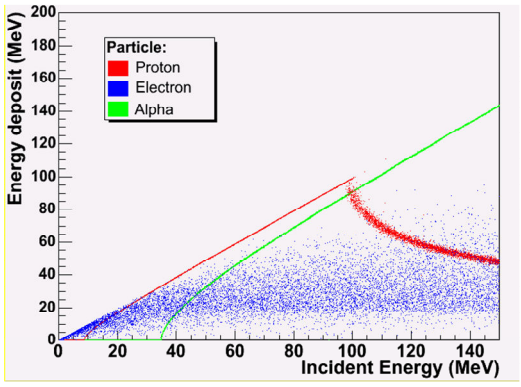

Fig. 3 Energy deposited in the crystal by electrons (blue dots), protons (red dots) and alpha particles (green dots), as a function of the energy of the incoming particle.

V. Fast Instrument Simulator using GEANT4 as a Benchmark

Geant4 was used as a benchmark in the derivation of transfer functions for a fast simulator of the instrument. The strategy chosen was to produce analytic functions describing the signals read by the electronics in each sub-detector, based on the geometry and on the physics processes involved. In the case of the trackers, these signals consist on the charge collected in each tracker plane, which is a function of the energy deposited by the incoming charged particles. In the

case of the crystal, the signal evaluation involves calculating the number of scintillating photons arriving at each PIN diode. The total number of scintillating photons emitted by a particle crossing the scintillator is proportional to the energy lost by the particle by a factor which is the scintillator light yield. In order to reduce the Geant4 simulation computing time, a light yield of 100 photons/MeV was used instead of the nominal value for the studied scintillator.

A. Crystal Transfer Functions

For the evaluation of the crystal transfer functions, only particles depositing all their energy in the detector (fully contained particles) were considered. In order to determine the particles containment, NIST range tables [7] were used. The transfer functions take as inputs the type of particle, the particle kinetic energy, its entry position on the crystal upper face and its incoming direction.

1) Transfer function for Protons in the Crystal

The signal in each PIN diode (crystal face) corresponds to the total number of scintillating photons arriving on its surface (hits). In its evaluation the solid angle factor of each crystal face, the reflections on the crystal upper face and the optical transmissivity between the crystal and the PIN diodes were considered. Therefore, the signal arriving on each PIN diode should be parameterised as:

$$Signal(face,P) = N_{photon}^{total} \cdot \rho 1 . k1(face) \times \left[\Omega(face,P) + k2(face)\rho 2 . S . \Omega(top,P)\right]$$

where P is a point belonging to the proton trajectory at which the solid angle covered by each PIN diode is calculated (optimised taking into account the shape of the energy loss distribution); N_{photon}^{total} is the total number of scintillating photons emitted by the proton; Ω(face,P) is the solid angle sub-intended by each face with respect to point P; ρ1 corresponds to the optical transmissivity between the crystal and the PIN diodes; Ω(top,P) is the solid angle sub-intended by the top crystal face (from where the particles come); ρ2 is the reflectivity of the top surface and S is a factor related to the solid angle sub-intended by the considered face with respect to the centre of the upper face (to take into account the probability of photons reflected in the upper surface to reach the other crystal faces); k1 and k2 are optimisation factors for each face. The total signal will therefore be obtained by summing up the signal collected by the five PIN diodes:

$$TotalSignal = \sum_{face=1}^{5} Signal(face)$$

An optimised transfer function, whose optimisation factors are listed in Table I, was derived using as a benchmark the Geant4 simulation of 1 MeV to 100 MeV protons crossing the detector, for an optical transmissivity between the crystal and the photodetectors ρ1=0.95 and a top surface reflectivity ρ2=0.95. The point at which the solid angle along the proton trajectory was calculated was optimized between the average value of the energy loss distribution and the final point of the proton trajectory. In order to compare the transfer function response with the Geant4 simulation, fiducial volume requirements had to be imposed to the simulated events. Therefore, it was required that the trajectory of a simulated in a proton inside the crystal ended 0.5 mm from the lateral walls and 1 mm from the top and bottom crystal faces.

TABLE 1

factor	Lateral faces	Bottom face
k1	0.970	1.000
k2	0.885	0.885

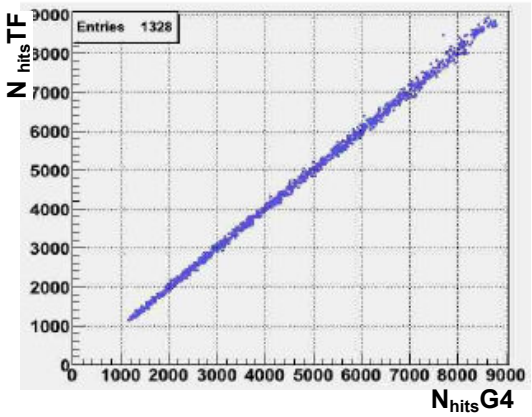

Fig. 4 Signal (number of photons) arriving to the 5 PIN diodes surrounding the crystal, evaluated with the transfer function versus the signal obtained with the Geant4 simulation, for the case where the incident particles are protons with energies ranging between 1 MeV and 100 MeV.

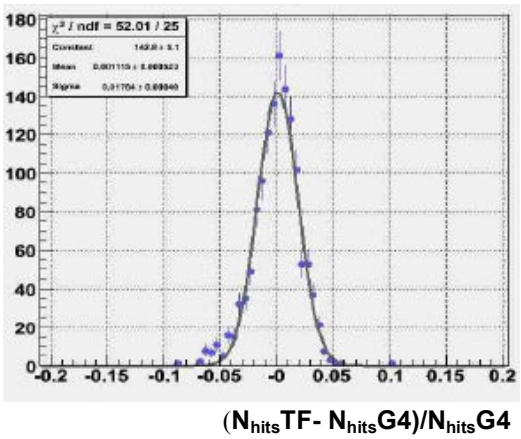

Fig. 5 Difference between the total signal collected by the 5 PIN diodes evaluated with the transfer function and with the Geant 4 detector simulation with respect to the signal obtained with Geant4, for the case where the incident particles are protons with energies ranging between 1 MeV and 100 MeV.

In figure 4 the total signal evaluated with the proton transfer function is compared with the same variable obtained with the Geant4 simulation. Figure 5 illustrates the difference between the transfer function and the Geant4 simulation, which is below 2%. This spread is dominated by the statistic uncertainty due to the number of scintillating photons produced in Geant4, lower than that produced in a realistic scintillator with a light yield 650 times higher.

2) Transfer Function for Alpha Particles in the Crystal

The analysis performed for alpha particles was similar to that performed for protons. The transfer function for alpha particles crossing the crystal makes use of the NIST range tables for alpha particles [7]. The transfer function parameters derived using a simulation of 1 MeV to 100 MeV protons, were found to be suitable for alpha particles.

In figure 6, the total signal in the PIN diodes, computed with the transfer function for alpha particles with energies ranging between 1 and 200 MeV, is compared to the result of the corresponding Geant4 simulation. The difference between the signal predicted by the transfer function and the signal obtained from the Geant4 simulation is, as in the case of protons, below 2%, (see figure 7).

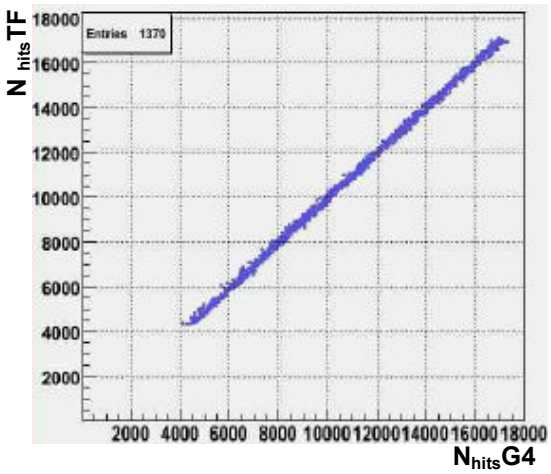

Fig. 6 Signal (number of photons) arriving to the 5 PIN diodes surrounding the crystal, evaluated with the transfer function versus the signal obtained with the Geant4 simulation, for incident alpha particles with energies ranging between 1 MeV and 200 MeV.

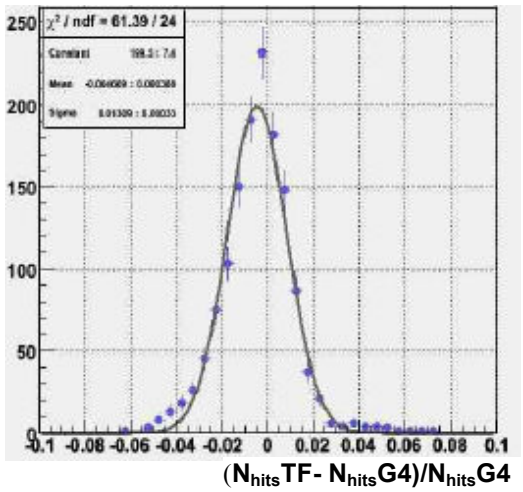

Fig. 7 Difference between the total signal collected by the 5 PIN diodes evaluated with the transfer function and with the Geant 4 detector simulation with respect to the signal obtained with Geant4, for incident alpha particles with energies ranging between 1 MeV and 200 MeV

3) Transfer Function f or Electrons in the Crystal

The case of electrons is more challenging than the previous cases due to the fact that for the range of energies studied, electrons radiate bremsstrahlung photons giving rise to showers inside the scintillator. Whether the radiated bremsstrahlung photons get absorbed or leave the scintillator carrying a possibly large part of the incident electron energy is crucial to the problem. Therefore, an analytic parameterisation of the photon cross-section for energies of the order of the tens of MeV is not a realistic approach to the problem. The solution found was to obtain probability distribution functions for the energy absorbed in the crystal as a function of the electron energy. These functions were derived from Geant4 simulations of mono-energetic electrons crossing the detector.

In figure 8 the total number of hits obtained from the transfer function (blue dots) is compared to the number of hits in the PIN diodes predicted by the Geant4 simulation (green dots) as a function of the kinetic energy of the electrons, for the case where no bremsstrahlung was considered in the transfer function, that is, the electron is considered to be fully absorbed and no radiation yield is used. As expected, the transfer function values maximize the Geant4 distribution for the full energy range.

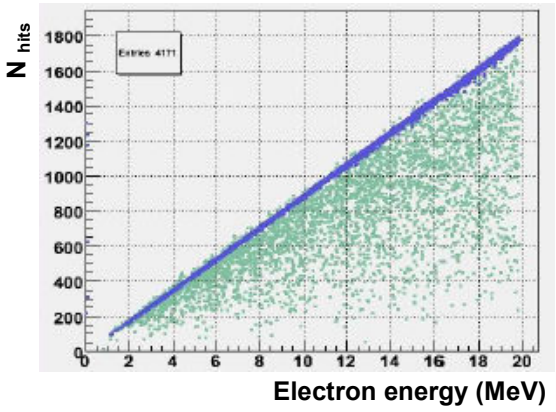

Fig. 8 Signal in the 5 PIN diodes as a function of the kinetic energy of the electrons entering the detector. The signal obtained with the transfer function is represented by the blue dots whereas the Geant4 simulation result is illustrated by the green dots. No bremsstrahlung was considered in the transfer function.

In figure 9, the same distributions are shown for the case where the radiation yield as a function of the electron energy, obtained from the NIST data base [7], is used in the transfer function to correct the energy absorbed in the crystal. In figure 10, the same distributions are compared for the case where the transfer function performs a random sampling of the electron absorbed energy making use of the parameterised electron absorbed energy probability distributions.

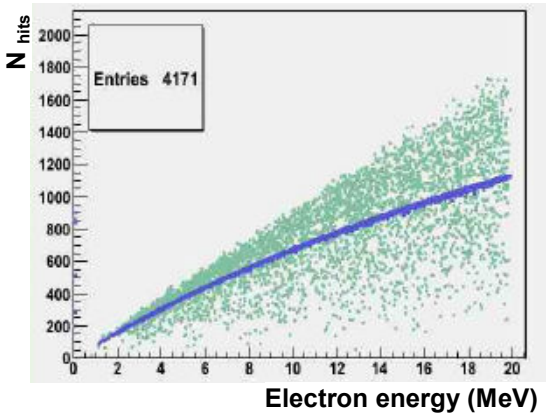

Fig. 9 Signal in the 5 PIN diodes as a function of the kinetic energy of the electrons entering the detector. The signal obtained with the transfer function is represented by the blue dots whereas the Geant 4 simulation result is illustrated by the green dots. Bremsstrahlung was introduced in the transfer function. The number of hits is obtained, in the transfer function, as the product of the electron energy (after radiation) by the crystal light yield.

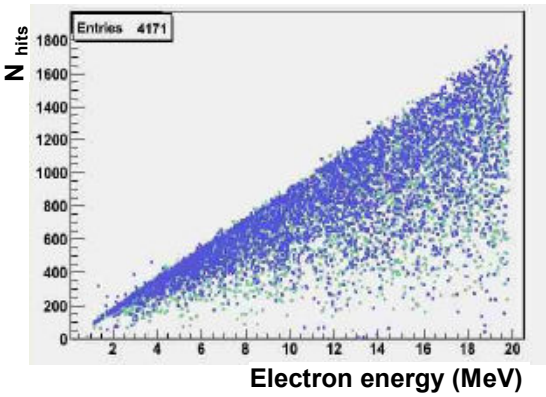

Fig. 10 Signal in the 5 PIN diodes as a function of the kinetic energy of the electrons entering the detector. The transfer function is represented by the blue dots whereas the Geant 4 simulation result is illustrated by the green dots. The transfer function takes into account bremsstrahlung and the number of hits in the transfer function is distributed according to a random distribution, obtained by a parameterisation of the Geant 4 output as a function of the electron energy.

In figures 11 and 12 the total signal in the 5 PIN diodes evaluated with the transfer function is compared to the corresponding output of the Geant4 simulation. The spread in the distribution in figure 17 is due to the width of the electron absorbed energy p.d.f.s and not to a poor transfer function performance.

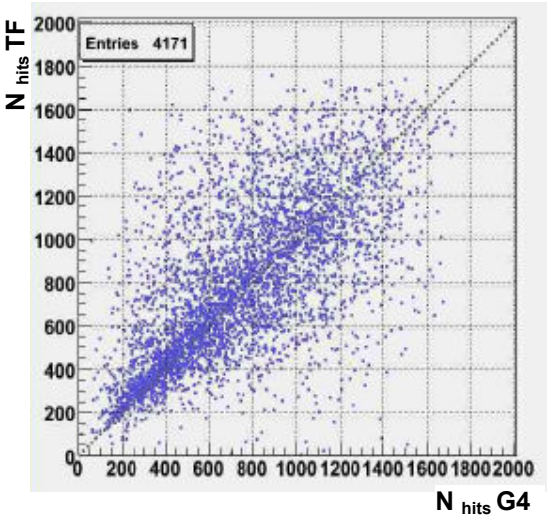

Fig. 11 Signal in the 5 PIN diodes obtained for electrons using the transfer function versus the signal obtained from the Geant4 simulation. The electron energies range between 0.1 MeV and 20 MeV.

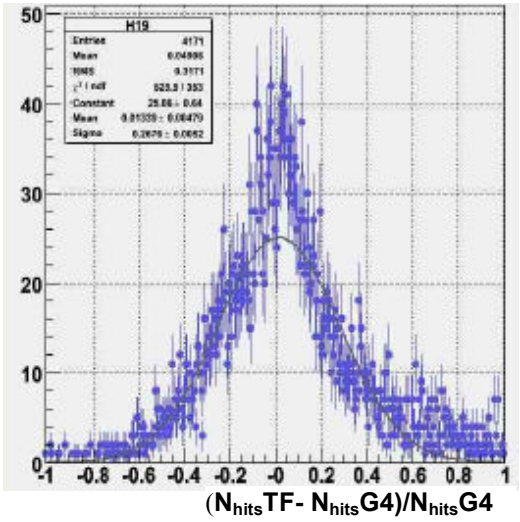

Fig. 12 Difference between the signal in the 5 PIN diodes, obtained with the electrons crystal transfer function and the number of detected scintillation photons in the corresponding Geant4 simulation.

A very good agreement was obtained between the transfer function for the signal left by electrons, protons and alpha particles in the scintillator and the corresponding Geant4 simulation results for the considered energy ranges.

B. Tracker Transfer Functions

The tracker transfer functions return the energy deposited in the trackers by the incoming particles, consisting of an evaluation of the energy loss in the trackers. This energy can then be converted to charge in a straightforward way.

The values of the energy lost by protons, alphas and electrons in the tracker planes were used in the crystal transfer functions, described previously, to corerst the energy of the particles when entering the crystal.

1) Tracker transfer functions for Protons and alpha particles

For the energy range studied, the approximation

$$\frac{dE}{dx} = C\beta^{-2}$$

is valid both for protons and alphas [8] and the average value for the energy lost in the trackers is evaluated from the inverse of:

$$\Delta x = \int \left(\frac{dE}{dx} \right)^{-1} dE$$

where Δx is the tracker thickness crossed by the particle. The constants C for protons and alpha particles were obtained from a fit to the Geant4 simulation results.

For protons and alpha particles in the studied energy range, the energy deposited in the trackers follows a Gaussian distribution with rms given by [9]:

$$\sigma = \sqrt{E_{\max} \xi \left(1 - \frac{\beta^2}{2} \right)}$$

$$E_{\max} = \frac{2 m_e \beta^2 \gamma^2}{1 + 2\gamma\, m_e / m_x + (m_e / m_x)^2}$$

$$\xi = 153.4 \frac{z^2}{\beta^2} \frac{Z}{A} \rho . \Delta x \ \text{keV}$$

where β is the particle velocity, m_e is the electron mass, m_x is the proton (or alpha particle) velocity, $\gamma = (1-\beta^2)^{-1}$, z is the charge of the incident particle, Z and A the atomic number and weight of the material , ρ its density and Δx is the material thickness crossed. Figures 13 and 14 show the comparison between the transfer function result for the energy lost in the first and second tracker planes (blue dots) and the Geant4 simulation results (green dots) for the case of protons. Figures 15 and 16 illustrate the corresponding comparisons for the case of alpha particles.

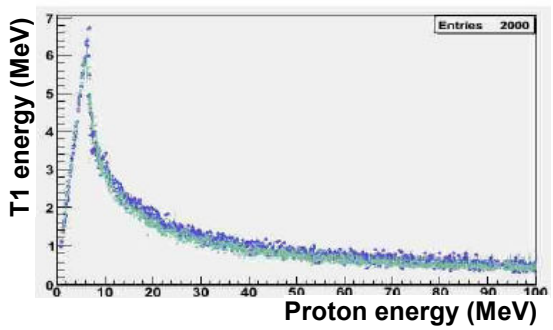

Fig. 13 Energy lost in the first Si tracker plane as a function of the proton energy. The green dots correspond to the Geant4 simulation, and the blue dots to the transfer function.

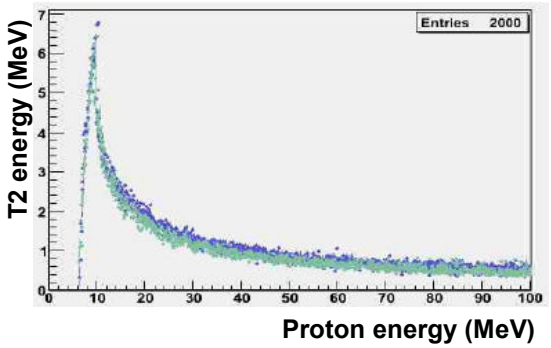

Fig. 14 Energy lost in the second Si tracker plane as a function of the proton energy. The green dots correspond to the Gean4 simulation, and the blue dots to the transfer function.

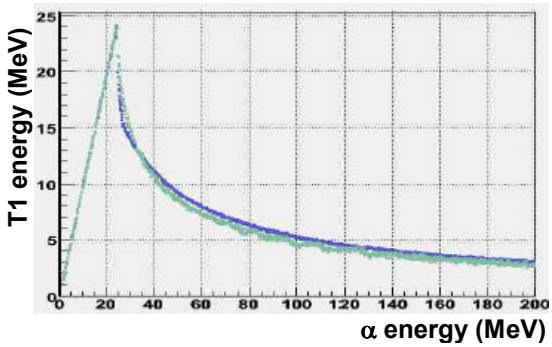

Fig. 15 Energy lost in the first Si tracker plane as a function of the energy of alpha particles. The green dots correspond to the Geant4 simulation, and the blue dots to the transfer function.

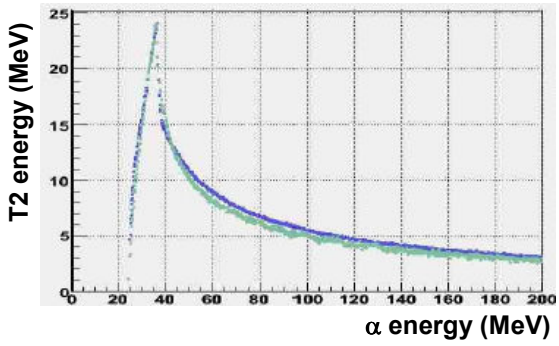

Fig. 16 Energy lost in the second Si tracker plane as a function of the energy of the alpha particles. The green dots correspond to the Geant4 simulation, and the blue dots to the transfer function.

2) Electrons Transfer Function for the Trackers

In the case of electrons, for the studied energy range the energy deposited in the trackers follows a Landau distribution [9]. The approximation used for the energy loss of protons and alphas is only valid for electrons with energies below ~1.6 MeV. As in the case of protons and alpha particles, the constant C was derived by adjusting the distribution to the Geant4 simulation results for the energy lost as a function of

the energy. For electron energies above 1.6 MeV the average value of the energy lost in the trackers was evaluated as:

$$\frac{dE}{dx}\Delta x$$

where dE/dx corresponds to Bethe-Bloch equation [8] and Δx is the tracker thickness crossed by the particles.

In figure 17 the energy lost by electrons in the first tracker plane evaluated with the transfer function (blue dots) is compared with the Geant4 simulation result (green dots). Figure 18 is a zoom of figure 17 in the electron energy range between 0.1 MeV and 4 MeV.

A good agreement was obtained between the trackers transfer function and the Geant4 simulation results for the energy lost by electrons, protons and alpha particles in the trackers.

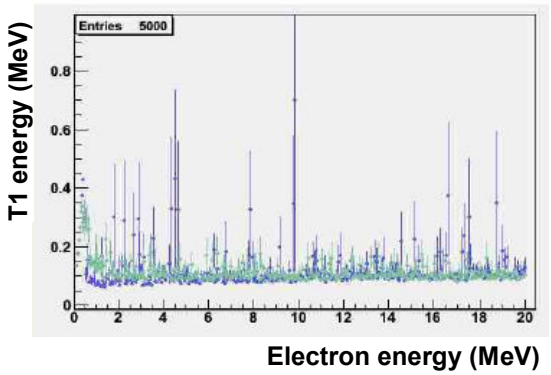

Fig. 17 Energy lost in the first Si tracker plane as a function of the electron energy. The green dots correspond to the Geant 4 simulation, and the blue dots to the transfer function.

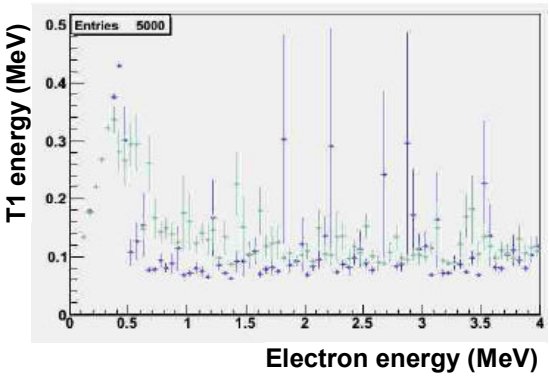

Fig. 18 Energy lost in the first Si tracker plane for electron energies ranging between 0.1 MeV and 4 MeV. The green dots correspond to the Geant4 simulation, and the blue dots to the transfer function.

VI. Conclusion

A new generation of compact, lightweight, general purpose radiation monitors needed for future space missions (e.g. Bepi Colombo) is under study. A simple concept based on a scintillating crystal was presented. The Instrument geometry and corresponding structural model were implemented in Geant4. The Geant4 toolkit proved to be a powerful tool both for a standalone simulation of the instrument and to be used as a benchmark for the development of a fast instrument simulator. Transfer functions for a fast instrument simulator were therefore developed, and a good agreement with the Geant 4 simulation results was obtained.

References

[1] E.R. Benton and E.V. Benton, "Space Radiation dosimetry in low-Earth orbit and beyond", *Nucl. Instrum. Methods* **B184**, 255 (2001).

[2] D. Maia, " Particles from the Sun", 5th international workshop on New Worlds in Astroparticle Physics, 8-10 January 2005, Universidade do Algarve – Faro, Portugal

[3] S. Agostinelli, J. Allison, K. Amako, J. Apostolakis, H. Araujo, P. Arce *et al.*, "GEANT4-a simulation toolkit", *Nucl. Instrum. Methods*, **506**, 250 (2003).

[4] M. G. Pia, "The Geant4 Toolkit: simulation capabilities and application results", *Nucl. Phys. B - Proc. Suppl.*, **125**, 60 (2003).

[5] A. Levin and C. Moisan, "A more physical approach to model the surface treatment of scintillation counters and its implementation in DETECT, in Proc. IEEE 1996 NSS, 2 (1996).

[6] A. Owens et al. (ESA-SCI/A), private communication.

[7] http://www.nist.gov, NIST,National Institute of Standards and Technology.

[8] http://pgd.lbl.gov, PDG, Particle Data Group.

[9] L.Landau, On the Energy loss of fast particles by Ionisation, J.Phys.,8:201.1944; S.M Seltzer and M.Berger, "Energy loss stragling of protons and mesons " In studies of penetration of charged particles in matte, Nucl.ScienceSeries39, Nat.Academy of Sciences,Washington DC, 1964.